A Collaborative RTK Approach to Precise Positioning for Vehicle Swarms in Urban Scenarios

Daniel Medina[1], Helena Calatrava[2], J. Manuel Castro-Arvizu[1], Pau Closas[2] and Jordi Vilà-Valls[3]

***Abstract*—Location information is fundamental in nowadays society and key for prospective driverless vehicles and a plethora of safety-critical applications. Global Navigation Satellite Systems (GNSS) constitute the main information supplier for outdoor positioning, with worldwide all-weather availability. While the use of GNSS carrier phase observations leads to precise location estimates, its performance can be easily jeopardized in urban scenarios, where satellite availability may be limited or observations may be corrupted by harsh propagation conditions. The satellite shortage is especially relevant for Real Time Kinematic (RTK), whose capability to estimate a precise positioning solution rapidly decays with weak observation models. To address this limitation, this article introduces the concept of collaborative RTK (C-RTK), an approach to precise positioning using swarms of vehicles, where a set of users participate in the vehicle network. The idea is that users with good satellite visibility assist users that evolve in constrained environments. This work introduces the C-RTK functional model, an estimation solution and associated performance bounds. Illustrative Monte Carlo simulation results are provided, which highlight that, by exploiting the cross-correlation terms present among the users' observations, C-RTK improves their positioning their of accuracy and availability.**

***Index Terms*—GNSS, Precise Positioning, Real Time Kinematic (RTK), Cooperative localization**

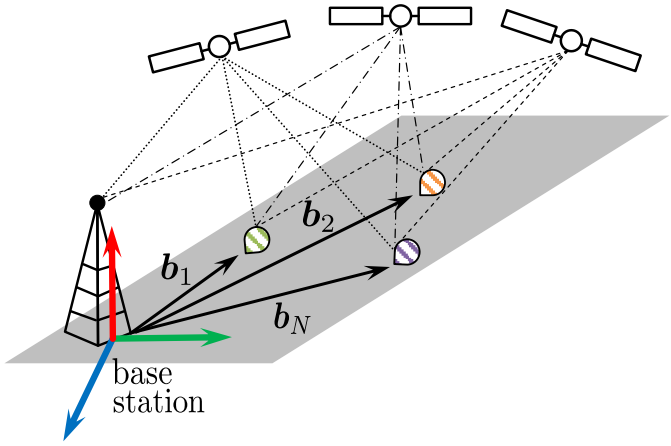

Fig. 1. Illustration for C-RTK: a set of nearby N users and a base station collect GNSS observations. The location of each of these $j = 1, \ldots, N$ users, $\boldsymbol{b}_j$, may be estimated locally by each of the users (standard RTK), or jointly estimated in a centralized manner (C-RTK). One of the major advantages of the proposed C-RTK approach is the provision of precise positioning to users that operate in constrained propagation conditions.

I. Introduction

Location-based services, as well as prospective intelligent transportation systems (i.e., driverless automobiles, unmanned ships, robots) entail reliable and precise positioning information for their successful operation [1]. Global Navigation Satellite Systems (GNSS) have become the gold standard and backbone for outdoor positioning and this dependence can only but grow in the future [2]. Typically, two types of GNSS ranging measurements can be exploited to obtain position, velocity and time (PVT) estimates (i.e., also Doppler measurements can be used, but they are not considered in this study [3], [4]): 1) code-based observations (pseudorange), derived from the apparent satellite signal time-of-flight; 2) carrier phase observations, derived from locally aligning a replica of the incoming signal and counting the cycles (time) elapsed over a temporal extent.

This work has been partially supported by the French DGA/AID under project 2022.65.0082 and the National Science Foundation under Award ECCS-1845833.

[1]Daniel Medina is with Institute of Communications and Navigation, German Aerospace Center (DLR), Neustrelitz, Germany. E-mail: daniel.ariasmedina@dlr.de; Juan Manuel Castro-Arvizu was with DLR at the time of this work.

[2]Helena Calatrava and Pau Closas are with Dept. of Electrical and Computer Eng., Northeastern University, Boston, MA (USA). E-mail: {calatrava.h, closas}@northeastern.edu

[3]Jordi Vilà-Valls is with ISAE-SUPAERO, University of Toulouse, Toulouse, France jordi.vila-valls@isae-supaero.fr

While code-based positioning constitutes the most extended GNSS commercial solution [5], with instantaneous solution of meter-level accuracy, its precision results deficient for modern applications. On the other hand, carrier phase-based positioning leads to a much higher precision, at the expense of estimating the unknown integer number of cycles, also called ambiguities. Based on the type of correction data used and the combination of observations, two precise positioning techniques are distinguished: Precise Point Positioning (PPP) and Real Time Kinematics (RTK), the first not being a real-time solution. This work focuses on RTK, a differential positioning approach for which the position of a target is estimated with respect to a nearby geolocated base station. Typically, the base station transmits the locally observed GNSS measurements to the target via Internet protocol and the target exploits these observations to eliminate the atmospheric and satellite-related delays. RTK approach is well established since the early 1990s, initially for surveying and geodetic purposes, with nearly instantaneous cm-level accuracies [2], [6], [7].

Nevertheless, RTK positioning performance can be easily jeopardized for various reasons, e.g., the separation between base and target is excessively large, multipath effects or limited/constrained satellite visibility. Some of the aforementioned challenges may be circumvented in various manners, for instance, long distance baselines can be palliated using partial ambiguity resolution techniques [8], [9], and multipath

2023 IEEE/ION Position, Location and Navigation Symposium (PLANS) | 978-1-6654-1772-3/23/$31.00 ©2023 IEEE | DOI: 10.1109/PLANS53410.2023.10139996

effects can be hindered with robust estimation [10], [11], beamforming [12], [13] or multi-sensor integration [14], [15]. Unfortunately, some of these solutions are challenging to implement at a mass-market level, due to its high computational and economical cost. Furthermore, the high structures present in deep urban environments obstruct the satellite visibility and constrain the overall GNSS coverage, for which the previous contributions do not provide a satisfactory answer.

Under these circumstances, the framework of collaborative localization in wireless sensor networks has emerged as a revolutionary alternative of ever-growing interest [16]–[18]. In this context, location-aware information is shared among the agents (users) of a network, or communicated to a central computing node, so that the overall positioning performance (for the complete set of users) is enhanced. When considering the perspective of inter-agent ranging enabled by new technologies, hybrid cooperative positioning will constitute a breakthrough for reliable and seamless localization [19]–[21]. Another interesting feature of such collaborative approach is that it may provide positioning capabilities to users of the network under harsh or GNSS-denied conditions [22]. While the benefits of GNSS-terrestrial collaborative localization networks have been successfully showcased, previous works focused solely in the use of GNSS code observations, which ignited this contribution.

This work introduces the concept of collaborative RTK (C-RTK), a network approach to RTK precise positioning, its observation functional model and the Cramér-Rao Bound (CRB) associated with its estimation problem. In C-RTK, the users of the network or vehicles of the swarm transmit their received GNSS observations to a central processing center (CPC), which also receives the observations from the nearest base station. Such CPC (i.e., which may be a master vehicle of the swarm) performs the standard double difference (DD) observation combination [2, Ch. 20] between the base and users' measurements and then jointly solves the position and integer ambiguities estimation for all users in the network. Once the solution is estimated, the CPC would transmit the users back with a precise positioning solution. A pictorial representation is shown in Figure 1.

Due to the DD combination with respect to the base station, the observations' noise model presents high cross-correlation among all users which, in turn, improves the integer estimation and leads to an enhanced positioning performance. Results based on an illustrative Monte Carlo simulation (refer to Section IV) demonstrate the promising performance of C-RTK, showcasing that the positioning improves with the number of network peers and, especially in scenarios with limited satellite coverage, extensively outperforms conventional RTK. The latter is one of the major advantages of the proposed C-RTK approach, where standalone vehicles that would be otherwise denied a precise positioning solution are now helped by the rest of vehicles operating under better propagation/visibility conditions.

The rest of the paper is organized as follows. Section II presents the basics of RTK positioning and introduces the C-RTK observation model. Section III is devoted to the estimation of the mixed model, both for RTK and C-RTK, as well as the associated estimation bounds. Finally, Sections IV and V present the simulation results and the conclusions of this work, respectively.

II. Collaborative RTK Model

In the following, the conventional RTK observation model is first detailed. Then, the C-RTK observation model is introduced and its stochastic modeling discussed.

A. RTK Observation Model

Let us consider that $n+1$ GNSS satellites are being simultaneously received over a single frequency at the j-th user and at a base station. At a particular time instance, the code and carrier phase observations for the i-th satellite measured at the j-th user are given by

$$\begin{aligned} \rho_j^i &= \|\boldsymbol{p}^i - \boldsymbol{p}_j\| + I^i + T^i + c\left(dt_j - dt^i\right) + \varepsilon_j^i, \\ \Phi_j^i &= \|\boldsymbol{p}^i - \boldsymbol{p}_j\| - I^i + T^i + c\left(dt_j - dt^i\right) + \lambda N_j^i + \epsilon_j^i, \end{aligned} \tag{1}$$

where the superscripts and subscripts make reference to the satellite and the user, respectively. Then, ρ and Φ are the code and carrier phase measurements, $\boldsymbol{p}_j$ and $\boldsymbol{p}^i$ are the user and satellite positions, I^i and T^i are the ionospheric and tropospheric delays, c is the speed of light, dt^i, dt_j are the satellite and user receiver clock offsets, λ is the carrier wavelength, N^i is the unknown number of cycles, and $\varepsilon^i, \epsilon^i$ are the noises containing the remaining unmodeled errors for the code and carrier phase observables.

To eliminate or disminish the atmospheric-related errors and the clock offsets, the DD combination integrates the n observations received at the base station and user with respect to an additional "pivot" satellite, as illustrated in Fig. 2. Thus, a particular DD combination between the i-th and r-th (pivot) satellite, base and user is as follows,

$$DD\rho_{j,m}^{i,r} = \rho_j^i - \rho_m^i - (\rho_j^r - \rho_m^r), \tag{2}$$

$$DD\Phi_{j,m}^{i,r} = \Phi_j^i - \Phi_m^i - (\Phi_j^r - \Phi_m^r), \tag{3}$$

and the complete vector of DD observations processed in conventional RTK results

$$\begin{aligned} \boldsymbol{y}_j &= \left[\boldsymbol{DD\Phi}j^\top, \boldsymbol{DD\rho}_j{}^\top\right]^\top \\ &= \left[DD\Phi_{j,m}^{1,r}, \ldots, DD\Phi_{j,m}^{n,r}, DD\rho_{j,m}^{1,r}, \ldots, DD\rho_{j,m}^{n,r}\right]^\top. \end{aligned} \tag{4}$$

The resulting observation model is denoted as *mixed* model, since the unknowns include real- and integer-valued parameters, and it is typically formulated following its linearized form as

$$\boldsymbol{y}_j \sim \mathcal{N}\left(\boldsymbol{A}\boldsymbol{a}_j + \boldsymbol{B}\boldsymbol{b}_j, \boldsymbol{\Sigma}_j\right), \text{with } \boldsymbol{a}_j \in \mathbb{Z}^n, \boldsymbol{b}_j \in \mathbb{R}^3, \tag{5}$$

where $\boldsymbol{b}_j = \boldsymbol{p}_j - \boldsymbol{p}_m$ represents the unknown j-th user position (with respect to the known base station position $\boldsymbol{p}_m$), and $\boldsymbol{a}_j$ is

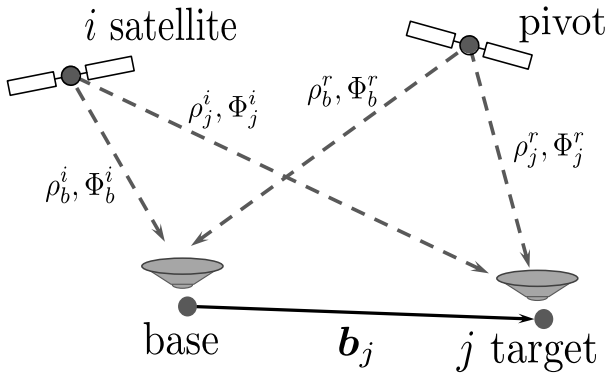

Fig. 2. Depiction of the satellites, base station and j-th target receiver involved in conventional RTK processing.

the vector of integer ambiguities. $\boldsymbol{A}$, $\boldsymbol{B}$ are the system design matrices

$$\boldsymbol{A} = \begin{bmatrix} \lambda \cdot \boldsymbol{I}_n \\ \boldsymbol{0}_n \end{bmatrix}, \ \boldsymbol{B} = \begin{bmatrix} \boldsymbol{DG} \\ \boldsymbol{DG} \end{bmatrix}, \ \boldsymbol{D} = \left[-\boldsymbol{1}_{n,1}, \boldsymbol{I}_n \right], \quad (6)$$

where $\boldsymbol{I}_n$ is the n-dimensional unit matrix, $\boldsymbol{0}_n$ is the n-dimensional null matrix and $\boldsymbol{1}_{n,1}$ is a column vector of ones. $\boldsymbol{D} \in \mathbb{R}^{n+1,n}$ is the double differencing matrix and $\boldsymbol{G} \in \mathbb{R}^{n,3}$ is the geometry matrix containing the satellite steering vectors [2, Ch. 21]. $\boldsymbol{\Sigma}_j$ represents the observations' covariance matrix and is described as

$$\boldsymbol{\Sigma}_j = \begin{bmatrix} 2 \cdot \sigma_\Phi^2 \cdot \boldsymbol{DW}^{-1}\boldsymbol{D}^\top & \\ & 2 \cdot \sigma_\rho^2 \cdot \boldsymbol{DW}^{-1}\boldsymbol{D}^\top \end{bmatrix}, \quad (7)$$

where σ_Φ, σ_ρ are the zenith-referenced standard deviation for the carrier phase and code observables, and $\boldsymbol{W}$ is a weighting matrix (typically dependent on the satellite elevation or the signal strength). Thus, RTK processing consists on solving the mixed model in (5) (i.e., estimate $\boldsymbol{b}_j$ and $\boldsymbol{a}_j$) to get a precise estimate on the j-th user's location.

B. Collaborative RTK Observation Model

Let us now assume that N users and a close-by base station simultaneously track $n+1$ satellites over a particular frequency. C-RTK assumes that all observations have been transmitted to a CPC in charge of estimating the positioning solution for the complete network of users. Thus, the C-RTK mixed model is cast as

$$\tilde{\boldsymbol{y}} \sim \mathcal{N}\left(\tilde{\boldsymbol{A}}\tilde{\boldsymbol{a}} + \tilde{\boldsymbol{B}}\tilde{\boldsymbol{b}}, \tilde{\boldsymbol{\Sigma}} \right), \text{with } \tilde{\boldsymbol{a}} \in \mathbb{Z}^{n \cdot N}, \tilde{\boldsymbol{b}} \in \mathbb{R}^{3 \cdot N}, \quad (8)$$

where $\tilde{\boldsymbol{y}} \in \mathbb{R}^{2 \cdot n \cdot N}$ stacks the DD carrier phase and code observations as

$$\tilde{\boldsymbol{y}} = \left[\boldsymbol{DD}\boldsymbol{\Phi}_1^\top, \ldots, \boldsymbol{DD}\boldsymbol{\Phi}_N^\top, \boldsymbol{DD}\boldsymbol{\rho}_1^\top, \ldots, \boldsymbol{DD}\boldsymbol{\rho}_N^\top \right]^\top, \quad (9)$$

and the vectors $\tilde{\boldsymbol{a}}, \tilde{\boldsymbol{b}}$ contain the unknown integer ambiguities and locations for the N users, such that

$$\tilde{\boldsymbol{a}} = \left[\boldsymbol{a}_1^\top, \ldots, \boldsymbol{a}_N^\top \right]^\top, \ \tilde{\boldsymbol{b}} = \left[\boldsymbol{b}_1^\top, \ldots, \boldsymbol{b}_N^\top \right]^\top, \quad (10)$$

and the design matrices are adapted consequently

$$\tilde{\boldsymbol{A}} = \begin{bmatrix} \boldsymbol{I}_N \otimes \lambda \cdot \boldsymbol{I}_n \\ \boldsymbol{I}_N \otimes \boldsymbol{0}_n \end{bmatrix}, \ \tilde{\boldsymbol{B}} = \begin{bmatrix} \boldsymbol{I}_N \otimes \boldsymbol{DG} \\ \boldsymbol{I}_N \otimes \boldsymbol{DG} \end{bmatrix}, \quad (11)$$

with $\otimes$ the Kronecker product. Finally, the C-RTK observations' covariance matrix $\tilde{\boldsymbol{\Sigma}}$ is described by

$$\tilde{\boldsymbol{\Sigma}} = \begin{bmatrix} \tilde{\boldsymbol{D}} \otimes \sigma_\Phi^2 \cdot \boldsymbol{DW}^{-1}\boldsymbol{D}^\top & \\ & \tilde{\boldsymbol{D}} \otimes \sigma_\rho^2 \cdot \boldsymbol{DW}^{-1}\boldsymbol{D}^\top \end{bmatrix}, \quad (12)$$

with $\tilde{\boldsymbol{D}}$ the mixing matrix to relate the base and users observations:

$$\tilde{\boldsymbol{D}} = \left[\boldsymbol{I}_N + \boldsymbol{1}_{N,N} . \right] \quad (13)$$

A relevant note is that, while the unknown parameters are completely uncorrelated among different users (unless inter-agent ranging measurements are available), the C-RTK covariance matrix introduces important cross-correlations. Since the DD combination is performed between each user and the base station, this additional information is of great importance, especially when the observation model is weak (e.g., when only a limited number of satellites are available). This occurrence is, indeed, very similar to the GNSS joint position and attitude estimation problem where this correlation was shown to bring significant advantages [23].

Another significant remark relates to the fact that users might neither track the same number nor the same satellites simultaneously. For instance, vehicles traversing urban scenarios, where the presence of skyscrapers and other high metallic structures predominate, would track a significant lower amount of satellites in comparison to other vehicles circulating in open sky conditions. In that case, the matrix dimensions for the elements of (8) shall be adapted accordingly, with the satellites in common across the network introducing the useful cross-correlations.

III. Collaborative RTK Estimation and Bounds

This section briefly explains the estimation problem of interest and the associated C-RTK estimation performance bound, in form of CRB.

A. Estimation Problem

The system of observations in (8) constitutes a complex optimization problem, due to the mixture of real and integer parameters. As for conventional RTK, a weighted least-squares formulation is as follows

$$\begin{bmatrix} \check{\boldsymbol{a}} \\ \check{\boldsymbol{b}} \end{bmatrix} = \arg \min_{(\boldsymbol{a},\boldsymbol{b}) \in \mathbb{Z}^{n \cdot N} \times \mathbb{R}^{3 \cdot N}} \left\| \tilde{\boldsymbol{y}} - \tilde{\boldsymbol{A}}\boldsymbol{a} - \tilde{\boldsymbol{B}}\boldsymbol{b} \right\|_{\tilde{\boldsymbol{\Sigma}}}^2, \quad (14)$$

where the notation $\tilde{\boldsymbol{a}}$ and $\tilde{\boldsymbol{b}}$ has been exchanged for $\boldsymbol{a}, \boldsymbol{b}$, respectively, for nomenclature simplicity. Due to the integer nature of $\boldsymbol{a}$, an explicit solution to (14) is not known. Instead, a three-step decomposition constitutes the most-widely applied solution approach [24], expressed as

$$\min_{\substack{\boldsymbol{a} \in \mathbb{Z}^{n \cdot N} \\ \boldsymbol{b} \in \mathbb{R}^{3 \cdot N}}} \|\tilde{\boldsymbol{y}} - \tilde{\boldsymbol{A}}\boldsymbol{a} - \tilde{\boldsymbol{B}}\boldsymbol{b}\|_{\tilde{\boldsymbol{\Sigma}}}^2 = \min_{\substack{\hat{\boldsymbol{a}} \in \mathbb{Z}^{n \cdot N} \\ \hat{\boldsymbol{b}} \in \mathbb{R}^{3 \cdot N}}} \|\tilde{\boldsymbol{y}} - \tilde{\boldsymbol{A}}\hat{\boldsymbol{a}} - \tilde{\boldsymbol{B}}\hat{\boldsymbol{b}}\|_{\tilde{\boldsymbol{\Sigma}}}^2 \quad (15a)$$

$$+ \min_{\boldsymbol{a} \in \mathbb{Z}^{n \cdot N}} \|\hat{\boldsymbol{a}} - \boldsymbol{a}\|_{\boldsymbol{P}_{\hat{\boldsymbol{a}}\hat{\boldsymbol{a}}}}^2 \quad (15b)$$

$$+ \min_{\boldsymbol{b} \in \mathbb{R}^{3 \cdot N}} \|\hat{\boldsymbol{b}}(\boldsymbol{a}) - \boldsymbol{b}\|_{\boldsymbol{P}_{\hat{\boldsymbol{b}}(\boldsymbol{a})}}^2, \quad (15c)$$

where (15a) disregards the integer constraints on the ambiguities and results in the so-called *float solution*. In terms of precision, the float solution aligns with that of differential code-based positioning, still insufficient for safety-critical applications. Then, (15b) constitutes an integer least squares (ILS) adjustment, where the real-valued ambiguities are mapped to integer ones. Finally, (15c) constitutes the *fixed solution*, which leads to high precision positioning by virtue of constraining the positioning solution based on the integer ambiguities. Note that, high precision positioning is reached only when the integer ambiguities are correctly estimated. For more details on the previous optimization problem, please refer to [2, Ch. 23]. In a nutshell, solving the C-RTK problem corresponds to the joint estimation of the individual RTK processes for every user, with the additional consideration of the cross-correlated noise. While the complexity and the search space increases moderately, the C-RTK performance improves the chances of finding the correct set of integer ambiguities, when compared to individual instances of RTK.

B. Bounds for Collaborative RTK

When considering an estimation problem, studying its associated performance bounds result fundamental to understand which is the best achievable (i.e., lower bounds) and the minimal (i.e., upper bounds) estimation performance. In the following, we shortly summarize the main results in [25]–[27], for the CRB of the mixed model, as well as the bootstrapped-based bound for integer estimation.

Let us denote with $\mathbf{CRB}_{\text{real}}$ the CRB matrix associated with the float positioning solution, given by

$$\mathbf{CRB}_{\text{real}} \triangleq \text{tr}\left([\boldsymbol{F}]^{-1}_{[1:3\cdot N, 1:3\cdot N]} \right), \qquad (16)$$
$$\boldsymbol{F} = \left[\tilde{\boldsymbol{B}}, \tilde{\boldsymbol{A}}\right]^{\top} \tilde{\boldsymbol{\Sigma}}^{-1} \left[\tilde{\boldsymbol{B}}, \tilde{\boldsymbol{A}}\right],$$

with $[\boldsymbol{F}]_{[1:3\cdot N, 1:3\cdot N]}$ denoting a submatrix of $\boldsymbol{F}$ comprising from the first to the $3N$-th rows and columns. The CRB for the positioning solution of the mixed model, $\mathbf{CRB}_{\text{mixed}}$, can be derived from [25] using the matrices and vectors in (8).

Similarly, understanding the performance of an estimator for the ILS is key to fully characterize the mixed model. Thus, the ILS success rate (i.e., the probability of correctly estimating the integer ambiguities) can be upper bounded by the performance of the bootstrapped integer estimator [28], as

$$P_s \triangleq P(\check{\boldsymbol{a}} = \boldsymbol{a}) = \prod_{i=1}^{n\cdot N} \left[2\,\Phi\left(\frac{1}{2\sigma_{\hat{a}'_i}} \right) - 1 \right], \qquad (17)$$

with $\Phi(\cdot)$ the cumulative normal distribution, and $\sigma_{\hat{a}'_i}$ the square-root for the diagonal values resulting from the lower-diagonal-upper decomposition of $\boldsymbol{P}_{\hat{\boldsymbol{a}}\hat{\boldsymbol{a}}}$ [27].

Taking into consideration the afore-described bounds, one can easily compare, in an analytical manner, the positioning performance of conventional RTK against C-RTK. Particularly, we aim at answering the following questions:

a) In open sky conditions, does the positioning accuracy improves with C-RTK?
b) Which is the RTK vs C-RTK performance in terms of probability of correctly estimating the integer solution?
c) If only a subset of users is affected by constrained propagation conditions, and the rest is in ideal open sky conditions, which is the RTK vs C-RTK performance for the constrained set?
d) Is the performance of C-RTK affected by the number of users conforming the collaborative network?

To answer these questions, we will resort to an illustrative Monte Carlo experimentation, where we will compare the estimation bounds of RTK and C-RTK against the performance of their estimators.

IV. Results

For the comparative performance assessment between RTK and C-RTK, an illustrative GNSS RTK experiment is simulated. A total of ten satellites (whose geometry is depicted in the skyplot of Fig. 3) are tracked by a base station of known location, with six vehicles receiving correction data from such station, and track a number of these satellites. Then, two study-cases are considered based on the number of tracked satellites by the vehicles: *i)* an open sky scenario where the network is fully connected, meaning that all vehicles and the base station simultaneously receive observations from the ten satellites (blue + red); *ii)* an urban scenario where two vehicles present a limited sky visibility and track four satellites (marked in red in Fig. 3), while the remaining users track the ten. Notice that this scenario is representative of a typical urban constrained satellite visibility environment.

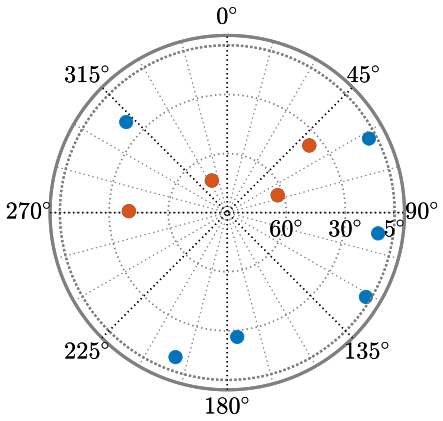

Fig. 3. Skyplot for the tracked satellites used for the simulated scenario. The red points correspond to the satellites tracked by the vehicles traversing an urban environment.

A range of precision levels is evaluated, such that the code zenith-referenced standard deviation varies from 0.01 m (i.e., an asymptotic case with very low noise) to 0.1 m (i.e., relatively high noise level). In all cases, the carrier phase zenith-referenced standard deviation is two orders of magnitude lower than the code counterpart. In addition, the noise across satellites is assumed to be identically distributed (therefore, the weighting matrix is set to $\boldsymbol{W} = \boldsymbol{I}$). For each

variation of noise level and case study, 1.000 Monte Carlo runs are performed to obtain statistically meaningful results.

A. Open Sky Scenario

Fig. 4 depicts the 3D position root mean squared error (RMSE) against the range of standard deviations for code measurements. The dashed blue and orange lines represent the CRB for the position estimate for a single user based on the mixed model for RTK and C-RTK, respectively, while the dashed black line depicts the CRB for the real-valued (i.e., float solution) signal model. Estimators are depicted with solid lines in blue and orange for conventional RTK and C-RTK, respectively.

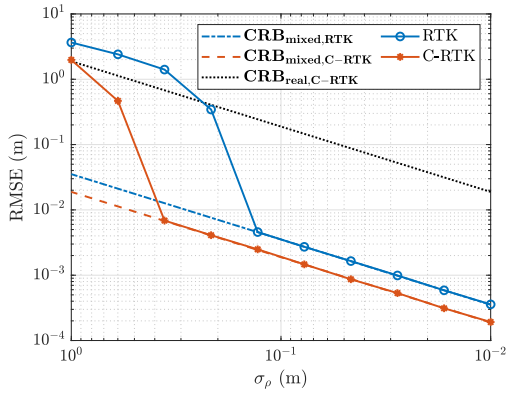

Fig. 4. Open sky scenario: positioning RMSE for estimators of the RTK and C-RTK models and square-root of CRBs as a function of the standard deviation of undifferenced code observables.

As extensively discussed in [25], [26], three regions of operation for the estimators' performance exist: asymptotic behaviour (where the ambiguities are correctly estimated and the resulting positioning solution presents high accuracy), a threshold region (where some integer ambiguities are wrongly estimated and introduce a bias on the solution), and a large noise regime (when the integer ambiguities cannot be correctly resolved and the inherent precision of carrier phase measurements is not exploited). In comparison to conventional RTK, the proposed C-RTK scheme poses two clear advantages: first, the accuracy of the positioning solution increases both for the float and fixed estimates; second, the asymptotic regime holds for a wider range of noise magnitudes.

A similar conclusion can be drawn from Fig. 5, which illustrates the experimental success ratio P_s –i.e., the chances for correctly estimating the integer ambiguities– of ILS estimators at the C-RTK and RTK models. For completeness, the ILS upper bound in (17) for the RTK and C-RTK problems (on black dashed and dotted lines, respectively) is also shown.

B. Urban Scenario

The second scenario covers the case in which certain vehicles (i.e., 2 out of 6) suffer from limited satellite coverage, while some other are in open sky conditions. Thus, this experiment aim at addressing whether C-RTK may enhance the chances to precisely locate vehicles in urban scenarios, that

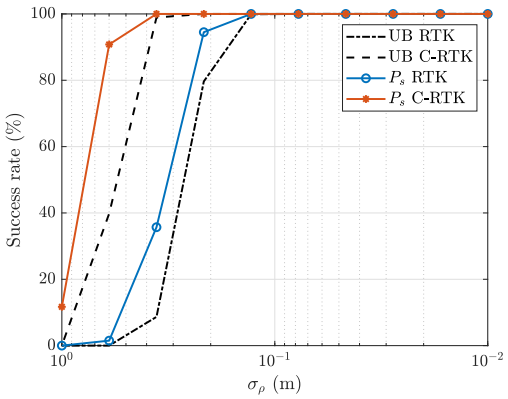

Fig. 5. Open sky scenario: experimental success rate P_s for RTK and C-RTK and associated ILS upper bounds against the magnitude of code noises.

is, if considering a vehicle swarm some of the vehicles in good operation conditions can help others that evolve under harsh environments. As for the previous section, the positioning RMSE and experimental success rate are depicted in Figs. 6 and 7, respectively, and make reference to the positioning performance for the vehicles with low/constrained satellite observability.

Fig. 6 shows a clear deterioration on the positioning performance when compared to the open sky scenario, with high precision localization being available only for low noise conditions. Still, C-RTK provides the same advantages w.r.t. conventional RTK that was already observed for the open sky scenario: the precision is increased and so are the chances to correctly estimate the integer ambiguities (Fig. 7).

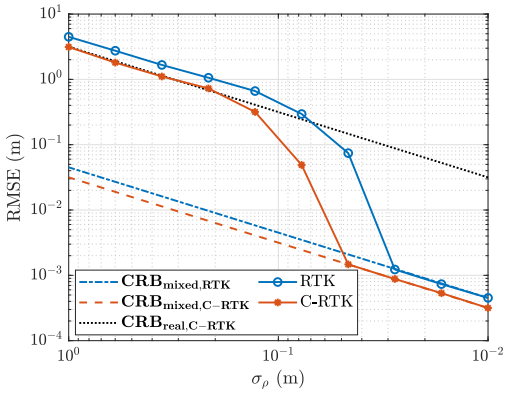

Fig. 6. Urban scenario: positioning RMSE for estimators of the RTK and C-RTK models and square-root of CRBs as a function of the standard deviation of undifferenced code observables.

More importantly, we suspect that such gain in positioning performance is related to the number of vehicles within the swarm, with the theoretical proof being part of the future work. Thus, a forthcoming scenario where vehicles are fully connected and the necessary data exchange possible, C-RTK has potential to overtake RTK as the standard method for high precision localization.

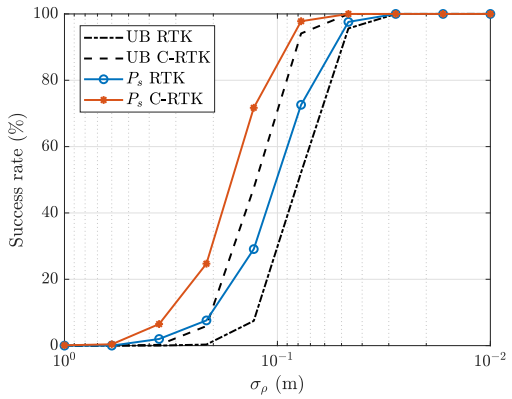

Fig. 7. Urban scenario: experimental success rate P_s for RTK and C-RTK and associated upper bounds for ILS as a function of the code noise.

V. Conclusions

This work studies how collaborative users can be leveraged to improve over RTK-based positioning. The basic principle is that the double differencing of observables that RTK performs, correlates the noise terms among nearby users. C-RTK constitutes an alternative technical solution to conventional RTK: instead of receiving corrections from a base station, the users in the network share their observations with the base station and a central computing node, the latter in charge of jointly estimating the positioning solution for all users. To gain understanding of the C-RTK processing, its functional model is introduced and the similarities to standard RTK showcased. Similarly, the estimation process and its associated estimation upper and lower bounds are discussed. From extensive Monte Carlo simulations we can conclude that C-RTK increases the positioning performance (in terms of precision) and the likelihood to correctly estimate the integer ambiguities. C-RTK exhibits its maximum potential for scenarios in which certain receivers in the collaborative set have low satellite coverage, with the remaining receivers featuring open sky conditions being able to "assist" the former in order to enable high precision localization..

References

[1] D. Dardari, P. Closas, and P. M. Djurić, "Indoor tracking: Theory, methods, and technologies," *IEEE Transactions on Vehicular Technology*, vol. 64, no. 4, pp. 1263–1278, 2015.

[2] P. J. G. Teunissen and O. Montenbruck, Eds., *Handbook of Global Navigation Satellite Systems*. Switzerland: Springer, 2017.

[3] F. Vincent, J. Vilà-Valls, O. Besson, D. Medina, and E. Chaumette, "Doppler-aided positioning in GNSS receivers-A performance analysis," *Signal Processing*, vol. 176, p. 107713, 2020.

[4] Y. J. Morton, F. Van Diggelen, J. J. Spilker, and B. W. Parkinson, Eds., *Position, Navigation, and Timing Technologies in the 21st Century: Integrated Satellite Navigation, Sensor Systems, and Civil Applications - Vol 1 and 2*. New Jersey, USA: Wiley-IEEE Press, 2021.

[5] F. Vincent, E. Chaumette, C. Charbonnieras, J. Israel, L. Ries, M. Aubourg, and F. Barbiero, "Asymptotically Efficient GNSS Trilateration," *Signal Processing*, vol. 133, pp. 270–277, April 2017.

[6] R. B. Langley, "RTK GPS," *GPS World*, vol. 9, no. 9, pp. 70–76, 1998.

[7] A. Heßelbarth, D. Medina, R. Ziebold, M. Sandler, M. Hoppe, and M. Uhlemann, "Enabling Assistance Functions for the Safe Navigation of Inland Waterways," *IEEE Intelligent Transportation Systems Magazine*, vol. 12, no. 3, pp. 123–135, 2020.

[8] A. Brack, "On reliable data-driven partial GNSS ambiguity resolution," *GPS solutions*, vol. 19, no. 3, pp. 411–422, 2015.

[9] J. M. Castro-Arvizu, D. Medina, R. Ziebold, J. Vilà-Valls, E. Chaumette, and P. Closas, "Precision-Aided Partial Ambiguity Resolution Scheme for Instantaneous RTK Positioning," *Remote Sensing*, vol. 13, no. 15, July 2021.

[10] H. Li, D. Medina, J. Vilà-Valls, and P. Closas, "Robust Variational-based Kalman Filter for Outlier Rejection with Correlated Measurements," *IEEE Transactions on Signal Processing*, 2020.

[11] D. Medina, H. Li, J. Vilà-Valls, and P. Closas, "Robust Filtering Techniques for RTK Positioning in Harsh Propagation Environments," *Sensors*, vol. 21, no. 4, p. 1250, 2021.

[12] G. Seco-Granados, J. A. Fernández-Rubio, and C. Fernández-Prades, "ML estimator and hybrid beamformer for multipath and interference mitigation in GNSS receivers," *IEEE Transactions on Signal Processing*, vol. 53, no. 3, pp. 1194–1208, 2005.

[13] E. P. Marcos, A. Konovaltsev, S. Caizzone, M. Cuntz, K. Yinusa, W. Elmarissi, and M. Meurer, "Interference and spoofing detection for GNSS maritime applications using direction of arrival and conformal antenna array," in *Proceedings of the 31st International Technical Meeting of The Satellite Division of the Institute of Navigation (ION GNSS+ 2018)*, 2018, pp. 2907–2922.

[14] M. Obst, S. Bauer, P. Reisdorf, and G. Wanielik, "Multipath detection with 3D digital maps for robust multi-constellation GNSS/INS vehicle localization in urban areas," in *IEEE Intelligent Vehicles Symposium*, 2012, pp. 184–190.

[15] G. Falco, M. Pini, and G. Marucco, "Loose and tight GNSS/INS integrations: Comparison of performance assessed in real urban scenarios," *Sensors*, vol. 17, no. 2, p. 255, 2017.

[16] N. Patwari, J. N. Ash, S. Kyperountas, A. O. Hero, R. L. Moses, and N. S. Correal, "Locating the nodes: cooperative localization in wireless sensor networks," *IEEE Signal Processing Magazine*, vol. 22, no. 4, pp. 54–69, 2005.

[17] H. Wymeersch, J. Lien, and M. Z. Win, "Cooperative localization in wireless networks," *Proceedings of the IEEE*, vol. 97, no. 2, pp. 427–450, 2009.

[18] A. Conti, M. Guerra, D. Dardari, N. Decarli, and M. Z. Win, "Network experimentation for cooperative localization," *IEEE Journal on Selected Areas in Communications*, vol. 30, no. 2, pp. 467–475, 2012.

[19] M. A. Caceres, F. Penna, H. Wymeersch, and R. Garello, "Hybrid cooperative positioning based on distributed belief propagation," *IEEE Journal on Selected Areas in Communications*, vol. 29, no. 10, pp. 1948–1958, 2011.

[20] D. Medina, L. Grundhöfer, and N. Hehenkamp, "Evaluation of Estimators for Hybrid GNSS-Terrestrial Localization in Collaborative Networks," in *IEEE 23rd International Conference on Intelligent Transportation Systems (ITSC)*, 2020.

[21] R. M. Buehrer, H. Wymeersch, and R. M. Vaghefi, "Collaborative sensor network localization: Algorithms and practical issues," *Proceedings of the IEEE*, vol. 106, no. 6, pp. 1089–1114, 2018.

[22] A. Naouri, L. Ortega, J. Vilà-Valls, and E. Chaumette, "A Multidimensional Scaling Approach for Cooperative GNSS Navigation," in *Intl. Conference on Localization and GNSS (ICL-GNSS)*, 2021.

[23] D. Medina, J. Vilà-Valls, A. Hesselbarth, R. Ziebold, and J. García, "On the Recursive Joint Position and Attitude Determination in Multi-Antenna GNSS Platforms," *Remote Sensing*, vol. 12, no. 12, p. 1955, 2020.

[24] P. J. G. Teunissen, "The Least-Squares Ambiguity Decorrelation Adjustment: A Method for Fast GPS Integer Ambiguity Estimation," *Journal of geodesy*, vol. 70, no. 1-2, pp. 65–82, 1995.

[25] D. Medina, J. Vilà-Valls, E. Chaumette, F. Vincent, and P. Closas, "Cramér-Rao Bound for a Mixture of Real- and Integer-Valued Parameter Vectors and Its Application to the Linear Regression Model," *Signal Processing*, vol. 179, 2021.

[26] D. Medina, L. Ortega, J. Vilà-Valls, P. Closas, F. Vincent, and E. Chaumette, "Compact CRB for Delay, Doppler and Phase Estimation – Application to GNSS SPP & RTK Performance Characterization," *IET Radar, Sonar & Navigation*, vol. 14, no. 10, pp. 1537–1549, Sep. 2020.

[27] A. Hassibi and S. Boyd, "Integer parameter estimation in linear models with applications to GPS," *IEEE Transactions on Signal Processing*, vol. 46, no. 11, pp. 2938–2952, 1998.

[28] P. J. Teunissen, "Success probability of integer GPS ambiguity rounding and bootstrapping," *Journal of Geodesy*, vol. 72, no. 10, pp. 606–612, 1998.